

---

# New Approach to Modeling the Direct Torque Control Applied to the Asynchronous Machine, Reduction of Undulations on the Torque

Hamid Yantour<sup>1</sup>, Janah Saadi<sup>2</sup>, Ahmed Khoumsi<sup>3</sup>

<sup>1</sup>Lab. of Automation and Production Engineering, ENSEM, Casablanca, Morocco

<sup>2</sup>Directeur Académique: Université Mohammed VI Polytechnique Lot 660, Hay Moulay Rachid 43150, Benguerir, Maroc

<sup>3</sup>Lab. Dept. Electrical & Computer Engineering, University of Sherbrooke, Canada

## Email address:

yantourhamid@gmail.com (H. Yantour)

## To cite this article:

Hamid Yantour, Janah Saadi, Ahmed Khoumsi. New Approach to Modeling the Direct Torque Control Applied to the Asynchronous Machine, Reduction of Undulations on the Torque. *International Journal of Intelligent Information Systems*. Special Issue: Smart Applications and Data Analysis for Smart Cities. Vol. 5, No. 3-1, 2016, pp. 5-22. doi: 10.11648/j.ijis.s.2016050301.12

**Received:** December 4, 2015; **Accepted:** January 5, 2016; **Published:** June 18, 2016

---

**Abstract:** In this paper, we study the Direct Torque Control (DTC) of an Induction Motor coupled to an Inverter (Inv-IM). DTC permits to control directly the stator flux and the torque by selecting the appropriate inverter state. DTC has been introduced because it presents several advantages in comparison to other techniques such as voltage/frequency control, vector control and field control. In this paper, we first model the DTC of Inv-IM as a hybrid system (HS). Then, we abstract the continuous dynamics of the HS in terms of discrete events. We thus obtain a discrete event model of the HS. And finally, we use Supervisory Control Theory of DES to drive Inv-IM to a desired working point.

**Keywords:** DTC, Automaton, DES, Controller, IM, Inv

---

## 1. Introduction

The main advantage of Induction motors (IM) is that no electrical connection is required between the stator and the rotor. Another advantage of IMs is that they have low weight and inertia, high efficiency and a high overload capability [1]. There exist several approaches to drive an IM. The Voltage/frequency (V/f) controller is the simplest technique, but its main disadvantage is its lack of accuracy in both speed and torque. Vector controllers are a technique that can reach a good accuracy, but its main disadvantages are the necessity of a huge computational capability and of a good identification of motor parameters [2]. The method of Field acceleration overcomes the computational problem of vector controllers by achieving some computational reductions [3], [2], [4]. And the technique of Direct Torque Control (DTC), that has been developed by Takahashi [5], [6], [7], [8], permits to control directly the stator flux and the torque by using an appropriate voltage vector selected in a look-up table. The main advantages of DTC are a minimal torque response time and the absence of: coordinate-transform,

voltage modulator-block, controllers such as PID for flux and torque. For these advantages, DTC is the control method adopted in this paper. Since the IM is driven through an inverter, the system to be controlled consists actually of the inverter and the IM and will be denoted Inv-IM. The latter is in fact a hybrid system, in the sense that it consists of a discrete component (the inverter) and a continuous component (IM). We propose a three-step method to model the DTC of Inv-IM and then drive Inv-IM to a desired working point.

- In a first step, we model the DTC of Inv-IM as a hybrid system (HS) with: a discrete event dynamics defined by the voltage vectors used to control IM; and a continuous dynamics defined by continuous equations on the stator flux vector  $\vec{\phi}_s$  and the electromagnetic torque  $\Gamma$ .
- In a second step, we abstract the continuous dynamics of the HS in terms of discrete events. Some events are used to represent the entrance and exit of the torque  $\Gamma$  and the amplitude  $\phi_s$  of  $\vec{\phi}_s$  in and from a working point region. And some other events are used to

represent the passage of the vector  $\vec{\varphi}_s$  between different zones. By this abstraction, the continuous dynamics of the system IM is described as a discrete event system (DES).

- In a third step, we use Supervisory Control Theory (SCT) [9], [18], [19], [20] to drive Inv-IM to a desired working point.

The remainder of the paper is structured as follows. Sect. 2 presents the inverter and its discrete event dynamics. Sect. 3 presents the induction motor and its continuous dynamics. In Sect. 4, we propose an abstraction of the continuous dynamics of the IM in terms of discrete events. Sect. 5 shows how to use SCT to drive Inv-IM to a targeted working point. In Sect. 6, we present the synthesis of the controller without reduction ripples on the torque and simulation results. The synthesis of the controller with reduction ripples on the torque and simulation results are presented in sect.7 and we conclude in sec.8.

## 2. Inverter and Its Discrete Event Model

The inverter (Figure 1) is supplied by a voltage  $U_0$  and contains three pair of switches ( $S_i^h, S_i^l$ ), for  $i = a, b, c$ . The input of the inverter is a three-bit value (SaSbSc) where each  $S_i$  can be set to 0 or 1. A value 0 of  $S_i$  sets ( $S_i^h, S_i^l$ ) to (close, open), and a value 1 sets it to (open, close). The output of the inverter is a voltage vector  $\vec{V}_s$  that drives IM.

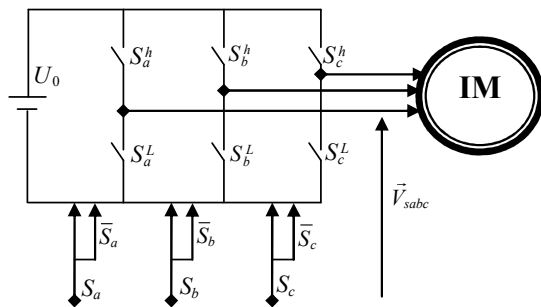


Figure 1. Inverter driving the induction motor.

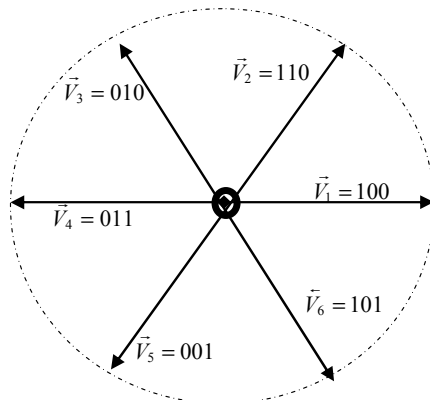


Figure 2. The six non-null voltage vectors in the reference frame fixed to the stator.

Equation (1) computes the voltage vector  $\vec{V}_s$  expressed in the  $\alpha$ - $\beta$  axes (i. e. the stationary reference frame fixed to the stator) after Concordia transformation. Note that  $\vec{V}_s$  depends uniquely on  $U_0$  and  $(S_c S_b S_a)$ , since  $U_0$  is fixed and  $(S_c S_b S_a)$  can have eight different values, we expect to obtain at most 8 voltage vectors. Actually, we have only 7 vectors, because the null vector is obtained for 000 and 111.

$$\vec{V}_s = \sqrt{\frac{2}{3}} U_0 [S_a + S_b e^{j\frac{2\pi}{3}} + S_c e^{j\frac{4\pi}{3}}] \quad (1)$$

The correspondence between  $\vec{V}_k$  and  $(S_c S_b S_a)$  is as follows:  $(\vec{V}_0, 000, 111)$ ,  $(\vec{V}_1, 001)$ ,  $(\vec{V}_2, 011)$ ,  $(\vec{V}_3, 010)$ ,  $(\vec{V}_4, 110)$ ,  $(\vec{V}_5, 100)$ ,  $(\vec{V}_6, 101)$ .

The inverter can be modeled by a 7-state automaton whose each state  $q_k$  ( $k = 0 \dots 6$ ) means: " $\vec{V}_k$  is the current voltage vector". Since  $\vec{V}_0$  can be obtained from the inputs 000 or 111 of the inverter, the selection between the two inputs can be done according to a specific control strategy. To adopt the terminology of hybrid systems, the term mode will be used as a synonym of state. The transition from any mode  $q_*$  to a mode  $q_k$  occurs by an event  $V_k$  which means "starting to apply  $\vec{V}_k$ ".

## 3. Induction Motor and its Continuous Model

The induction motor is a continuous system because its behavior is modeled by algebraic and differential equations on two continuous variables: the stator flux  $\varphi_s$  and the electromagnetic torque  $\Gamma$ . For conciseness, by flux we mean stator flux, and by torque we mean electromagnetic torque.

### 3.1. Model of Flux and Torque

With DTC, the voltage vector  $\vec{V}_s$  generated by the inverter is applied to the IM to control the flux  $\varphi_s$  and the torque  $\Gamma$ . Let us first see how  $\varphi_s$  and  $\Gamma$  can be expressed. In a stationary reference frame, the flux vector  $\vec{\varphi}_s$  is governed by the differential Eq. (2), where  $R_s$  is the stator resistance and  $\vec{I}_s$  is the stator current vector. Under the assumption that  $R_s \vec{I}_s$  is negligible w. r. t.  $\vec{V}_s$  (realistic if the amplitude of  $\vec{\varphi}_s$  is sufficiently high), we obtain Eq. (3) which approximates the evolution of  $\vec{\varphi}_s$  from  $\vec{\varphi}_{s0}$  after a delay  $t$ .

$$\vec{V}_s = R_s \vec{I}_s + \frac{d\vec{\varphi}_s}{dt} \quad (2)$$

$$\vec{\varphi}_s = \vec{\varphi}_{s0} + \vec{V}_s \cdot t \quad (3)$$



combinations of the evolution of  $(\varphi_s, \Gamma)$  (see Table 1).

**Table 2.** Evolution of  $\varphi_s$  and  $\Gamma$  under the control of  $\vec{V}_i$  and  $\vec{V}_{i+3}$ .

	$\vec{V}_i$	$\vec{V}_{i+3}$
$\varphi_s$	↑	↓
$\Gamma$	↑ if j=1 ↓ if j=2	↓ if j=1 ↑ if j=2

A second approach to solve the nondeterminism is to use twelve zones by dividing each  $z_i$  into two zones  $z_{i,1}$  and  $z_{i,2}$  comprising the first and the second 30 degrees, respectively [13], [1]. Figure 5 represents the twelve-zone division. In each zone  $z_{i,j}$  and under the control of  $\vec{V}_{i-2}, \vec{V}_{i-1}, \vec{V}_{i+1}, \vec{V}_{i+2}$  and  $\vec{V}_0$ , the evolution of  $\varphi_s$  and  $\Gamma$  is thus the one already indicated in Table 1. Table 2 shows the evolution of  $\varphi_s$  and  $\Gamma$  in zone  $z_{i,j}$  under the control of  $\vec{V}_i$  and  $\vec{V}_{i+3}$ .

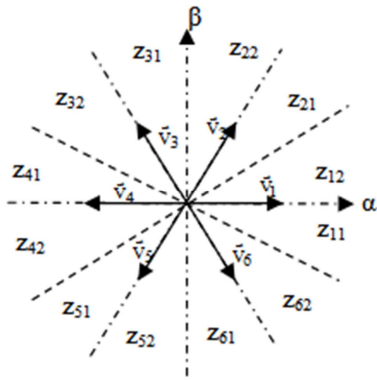


**Figure 5.** Locus of  $\vec{\varphi}_s$  divided into twelve zones.

## 4. IM modeled as a DES by Abstracting Its Continuous Dynamics

Let us show how the continuous dynamics of IM presented in Sect. 3 is abstracted in terms of discrete events. The first abstraction consists in translating by events the entrance and exit of  $(\varphi_s, \Gamma)$  in and from a working point region. The second abstraction consists in translating by events the passage of the vector  $\vec{\varphi}_s$  between orientation zones.

### 4.1. Abstracting the Entrance and Exit of $(\varphi_s, \Gamma)$ in and from a Working Point Region

Let  $\varphi_{wp}$  and  $\Gamma_{wp}$  be the flux magnitude and the torque defining the targeted working point. That is, the aim of control will be to drive IM as close as possible to  $(\varphi_{wp}, \Gamma_{wp})$ . We define a flux interval  $[\varphi_{wp}^-, \varphi_{wp}^+]$  centered in  $\varphi_{wp}$ , and a torque interval  $[\Gamma_{wp}^-, \Gamma_{wp}^+]$  centered in  $\Gamma_{wp}$ . We partition the space of  $(\varphi_s, \Gamma)$  into sixteen regions  $R_{u,v}$ , for  $u, v = 1, 2, 3, 4$ , as shown in Figure 6. The objective of the

control will be to drive IM into the set of regions  $\{R_{u,v} : u, v = 2, 3\}$  and to force it to remain into this set. We define the event  $\varphi_u^u$  that represents a transition from  $R_{u,v}$  to  $R_{u',v}$  for any  $v$ , and the event  $\Gamma_v^v$  that represents a transition from  $R_{u,v}$  to  $R_{u,v'}$  for any  $u$ . Since only transitions between adjacent regions are possible, the unique possible events are the following:  $\varphi_u^{u+1}$  if  $u < 4$ ,  $\varphi_u^{u-1}$  if  $u > 1$ ,  $\Gamma_v^{v+1}$  if  $v < 4$ , and  $\Gamma_v^{v-1}$  if  $v > 1$ .

With the above abstraction, the evolution of  $(\varphi_s, \Gamma)$  can be described by a 16-state automaton, whose states are noted  $\langle u, v \rangle$  and correspond to the sixteen regions  $R_{u,v}$ ,  $u, v = 1, 2, 3, 4$ . The transitions between states occur with the events defined above:  $\varphi_u^{u+1}, \varphi_u^{u-1}, \Gamma_v^{v+1}, \Gamma_v^{v-1}$ .

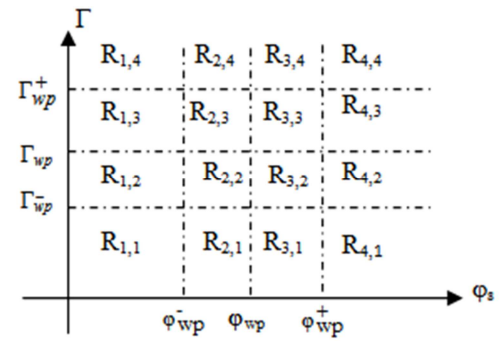


**Figure 6.** Partitioning of the space of  $(\varphi_s, \Gamma)$ .

### 4.2. Abstracting the Passage of $\vec{\varphi}_s$ Between Orientation Zones

In Sections. 3-2 and 3-3, we have shown how to partition the global locus of  $\vec{\varphi}_s$  into six or twelve zones (Figures 4 and 5). This partitioning is very relevant, because we have seen that from the knowledge of the current zone occupied by  $\vec{\varphi}_s$ , we can determine the control vector  $\vec{V}_k$  to be applied for obtaining a given evolution of  $(\varphi_s, \Gamma)$  (Tables I and II).

With the 6-zone partition, we define the event  $z_i^i$  that represents a transition from  $z^i$  to  $z^{i'}$ . Since only transitions between adjacent zones are possible, the unique possible events are the following:  $z^{i+1}, z^{i-1}$ , where  $i-1$  and  $i+1$  are defined modulo 6. We can thus abstract the evolution of  $\vec{\varphi}_s$  by a 6-state automaton, whose states are noted  $\langle i \rangle$  and correspond to the zones  $z_i$ ,  $i = 1, \dots, 6$ . The transitions between states occur with the events defined above:  $z_i^{i+1}, z_i^{i-1}$ .

We can use the same approach with the 12-zone partition, by defining the event  $z_{i,j}^{i',j'}$  that represents a transition from

$z_{i,j}$  to  $z_{i',j'}$ . Since only transitions between adjacent zones are possible, the unique possible events are the following:  $z_{i,1}^{i,2}$ ,  $z_{i,2}^{i,1}$ ,  $z_{i,1}^{i-1,2}$ ,  $z_{i,2}^{i+1,1}$ , where  $i-1$  and  $i+1$  are defined modulo 6. We can thus abstract the evolution of  $\bar{\varphi}_s$  by a 12-state automaton, whose states correspond to the zones  $z_{i,j}$ ,  $i = 1, \dots, 12$  and  $j = 1, 2$ . The transitions between states occur with the events defined above:  $z_{i,1}^{i,2}$ ,  $z_{i,2}^{i,1}$ ,  $z_{i,1}^{i-1,2}$ ,  $z_{i,2}^{i+1,1}$ .

### 4.3. Modeling IM As a DES

In Sect. 4-1, we have shown how to abstract the evolution of  $(\varphi_s, \Gamma)$  by a 16-state automaton. In Sect. 4-2, we have shown how to abstract the evolution of  $\bar{\varphi}_s$  by a 6-state or 12-state automaton. In the sequel, we consider uniquely the 6-state automaton because it reduces the state space explosion which is inherent to the use of automata. As we have seen in Sect. 3-3, the 6-zone partition necessitates to apply a control vector different from  $\bar{V}_1$  and  $\bar{V}_{i+3}$ , when  $\bar{\varphi}_s$  is in  $z_i$ . We will explain in Sect.5 how this requirement can be guaranteed by supervisory control of DES. Let us see how the two automata (16-state and 6-state) are combined into an automaton Mk that abstracts the behavior of IM when a given control vector  $\bar{V}_k$  is applied by the inverter. A State of Mk is noted  $\langle u, v, i \rangle k$  since it is a combination of a state  $\langle u, v \rangle$  (corresponding to  $R_u, \Gamma$ ) and a state  $\langle i \rangle$  (corresponding to  $z_i$ ). Mk can therefore have at most  $6 \times 16 = 96$  states  $\langle u, v, i \rangle k$ , ( $u, v = 1, \dots, 4$ ,  $i = 1, \dots, 6$ ). By interpreting Table I, we determine the transitions of Mk as follows, where  $\bar{V}_k$  is the control vector currently applied by the inverter. From state  $\langle u, v, i \rangle k$  of  $M_k$ :

- The event  $\varphi_u^{u+1}$  can occur when  $u < 4$  and  $\varphi_s$  increases, i.e., when  $k$  is equal to one of the following values:  $i-1$ ,  $i+1$ ,  $i$ . this event  $\varphi_u^{u+1}$  leads from  $\langle u, v, i \rangle k$  to  $\langle u+1, v, i \rangle k$ .
- The event  $\varphi_u^{u-1}$  can occur when  $u > 1$  and  $\varphi_s$  decreases, i.e., when  $k$  is equal to one of the following values:  $i-2$ ,  $i+2$ ,  $i+3$ . This event  $\varphi_u^{u-1}$  leads from  $\langle u, v, i \rangle k$  to  $\langle u-1, v, i \rangle k$ .
- The event  $\Gamma_v^{v+1}$  can occur when  $v < 4$  and  $\Gamma$  increases, i. e., when  $k$  is equal to one of the following values:  $i+1$ ,  $i+2$ ,  $i$ ,  $i+3$ . This event  $\Gamma_v^{v+1}$  leads from  $\langle u, v, i \rangle k$  to  $\langle u, v+1, i \rangle k$ .
- The event  $\Gamma_v^{v-1}$  can occur when  $v > 1$  and  $\Gamma$  decreases, i. e., when  $k$  is equal to one of the following values:  $i-2$ ,  $i-1$ ,  $i$ ,  $i+3$ ,  $0$ . This event  $\Gamma_v^{v-1}$  leads from  $\langle u, v, i \rangle k$  to  $\langle u, v-1, i \rangle k$ .
- The event  $z_i^{i+1}$  can occur when  $\bar{\varphi}_s$  rotates

counterclockwise, i. e., when  $\Gamma$  increases, i. e., when  $k$  is equal to one of the following values:  $i+1$ ,  $i+2$ ,  $i$ ,  $i+3$ .

This event  $z_i^{i+1}$  leads from  $\langle u, v, i \rangle k$  to  $\langle u, v, i+1 \rangle k$ .

- The event  $z_i^{i-1}$  can occur when  $\bar{\varphi}_s$  rotates clockwise, i. e., when  $\Gamma$  decreases, i. e., when  $k$  is equal to one of the following values:  $i-2$ ,  $i-1$ ,  $i$ ,  $i+3$ ,  $0$ . this event  $z_i^{i-1}$  leads from  $\langle u, v, i \rangle k$  to  $\langle u, v, i-1 \rangle k$ .

Due to the nondeterminism related to  $\bar{V}_i$  and  $\bar{V}_{i+3}$  (explained in Sect. 3-2 and in the second Table I), the events depending on the evolution of  $\Gamma$  ( $\Gamma_v^{v+1}$ ,  $\Gamma_v^{v-1}$ ,  $z_i^{i+1}$ ,  $z_i^{i-1}$ ) are potential but not certain when  $k$  is equal to  $i$  or  $i+3$ .

## 5. Use of SCT to Drive Im to a Working Point

### 5.1. Introduction to Supervisory Control

In this section, we show how to use Supervisory Control Theory (SCT) [9] to drive IM to a desired working point. In supervisory control, a supervisor Sup interacts with a DES (called plant) and restricts its behavior so that it respects a specification [9]. An important study in SCT is to synthesize a supervisor Sup when the plant and the specification are given and defined by two FSA P and S, respectively [9]. Sup observes the evolution of P (i. e., the events executed by the plant) and permits only the event sequences accepted by S. To achieve its task, Sup will disable (i. e., prevent) and force events. The concept of controllable event has thus been introduced, meaning that when an event  $e$  is possible, then Sup can disable it if and only if  $e$  is controllable;  $e$  is said uncontrollable if it is not controllable [9]. We will also use the notion of forcible event, meaning that when an event  $e$  is possible, then Sup can force  $e$  to preempt (i. e., to occur before) any other possible event, if and only if  $e$  is forcible;  $e$  is said unforcible if it is not forcible [14]. A method has been proposed to synthesize Sup automatically from P, S and the controllability and forcibility of every event [9].

### 5.2. The Plant Inv-IM Modeled As a DES

The plant to be controlled is the system Inv-IM (i. e., inverter with IM). In Section 2, we have modeled the inverter by an automaton A with 7 states  $q_k$  ( $k = 0, \dots, 6$ ) corresponding to the 7 control vectors  $\bar{V}_k$ , respectively. And in Section 4-3, when a given  $\bar{V}_k$  is applied by the inverter to the IM, we have modeled the evolution of IM by an automaton Mk that can have at most  $6 \times 16 = 96$  states  $\langle u, v, i \rangle k$ , ( $u, v = 1, \dots, 4$ ,  $i = 1, \dots, 6$ ). Therefore, the system Inv-IM can be modeled by replacing in A each mode  $q_k$  by the automaton Mk. The transition from any state  $\langle u, v, i \rangle k$  to a state  $\langle u, v, i \rangle k$  occurs by an event  $V_k$ . The obtained automaton, noted P, can therefore have at most  $7 \times 96 = 672$  states. The initial state is  $\langle 1; 1; 1 \rangle 0$ , that is, initially: the flux and the torque are in

Region R1, 1, the flux vector is in zone z1 and the null control vector  $\vec{V}_0$  is applied. The set of marked states is  $\{(u; v; i)k: u, v = 2, 3\}$ , because the objective of the control is to drive Inv-IM into the set of regions  $\{Ru, v: u, v = 2, 3\}$  (i. e., the set of states  $\{(u; v; i)k: u, v = 2, 3\}$ ), and then to force it to remain into this set. For the purpose of control, we define an undesirable event Null meaning that the flux or the torque has decreased to zero, and a state E reached with the occurrence of Null. We will see later how Null and E are necessary. Therefore, the automaton P has actually at most 673 (672 + the state E), and its alphabet  $\Sigma$  is:

$$\Sigma = \left\{ \phi_u^{u+1}, \Gamma_v^{v+1} : u, v = 1, 2, 3 \right\} \cup \left\{ \phi_u^{u-1}, \Gamma_v^{v-1} : u, v = 2, 3, 4 \right\} \\ \cup \left\{ Z_i^{i+1}, Z_i^{i-1} : i = 1, \dots, 6 \right\} \cup \left\{ V_k : k = 1, \dots, 6 \right\} \cup \text{null}$$

### 5.3. Control Architecture

We propose the control architecture illustrated in Figure 7. The interaction between the plant and the supervisor is realized through two interfaces A and G:

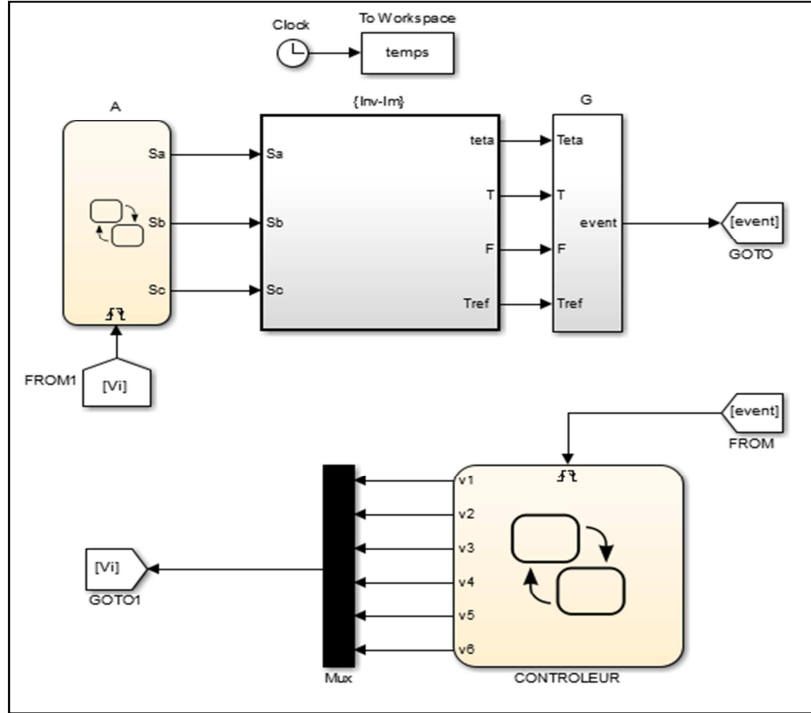


Figure 7. Control architecture, interaction between the plant and the supervisor.

A: In Sect.2, we have modeled the inverter by an automaton executing the events  $V_k$ ,  $k = 0 \dots 6$ . The interface A translates every event  $V_k$  generated by the supervisor into (SaSbSc), using the following correspondence (already given in Section 2):

$(\vec{V}_0, 000, 111)$ ,  $(\vec{V}_1, 001)$ ,  $(\vec{V}_2, 011)$ ,  $(\vec{V}_3, 010)$ ,  $(\vec{V}_4, 110)$ ,  $(\vec{V}_5, 100)$ ,  $(\vec{V}_6, 101)$ . And the inverter translates (SaSbSc) into the control vector  $\vec{V}_k$ , which is applied to IM.

G: In Sect. 4, we have modeled IM by an automaton executing the events  $Z_i^i$ ,  $\phi_u^u$ ,  $\Gamma_v^v$ . And in Sect. 5.2, we have added an event Null in the model of IM. The interface G generates these events as follows:  $Z_i^i$  is generated when  $\vec{\phi}_s$  passes from  $z_i$  to  $z_i'$ ;  $\phi_u^u$  is generated when  $\phi_s$  passes from  $R_u$ ,  $\star$  to  $R_u', \star$ ;  $\Gamma_v^v$  is generated when  $\Gamma$  passes from  $R_\star, v$  to  $R_\star, v'$ ; Null when  $\phi_s$  or  $\Gamma$  reaches the value zero.

The system  $\{\text{Inv-IM}, A, G\}$  forms the plant modeled by

the 672-state automaton P of Sect.5-2. With this architecture:

- Sup observes the events  $Z_i^i$ ,  $\phi_u^u$ ,  $\Gamma_v^v$ . Since these events are generated by IM through G, Sup has no control on them. Hence, these events are uncontrollable and unforcible.
- Sup generates the events  $V_k$ , and thus, has all control on them. Hence, these events are controllable and forcible.

We use the following hypothesis: Hypothesis 5.1: The plant is slow in comparison to Sup, in the sense that Sup can always force an event  $V_k$  to preempt any possible event  $Z_i^i$ ,

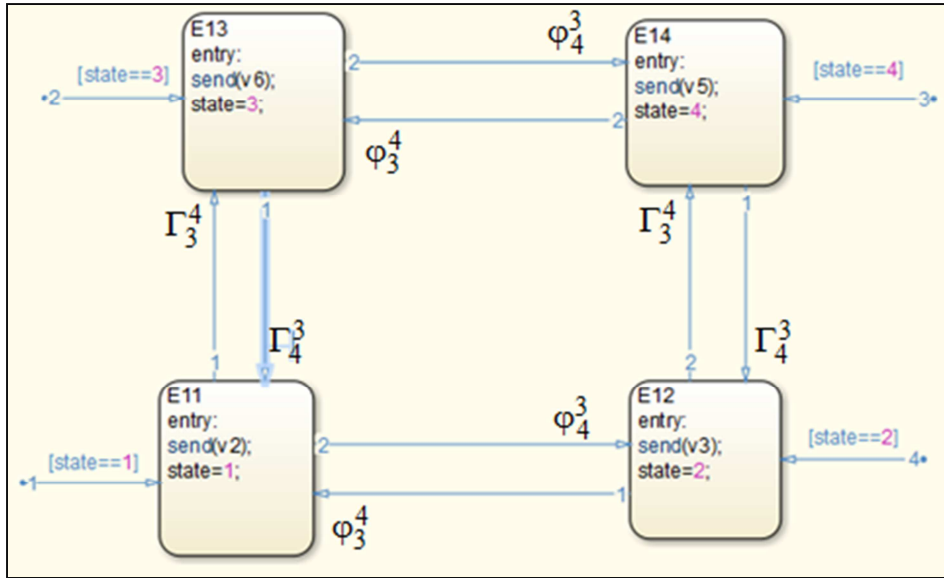
$$\phi_u^u, \Gamma_v^v.$$

## 6. Synthesis of the Controller Without Reduction of Ripples on the Torque

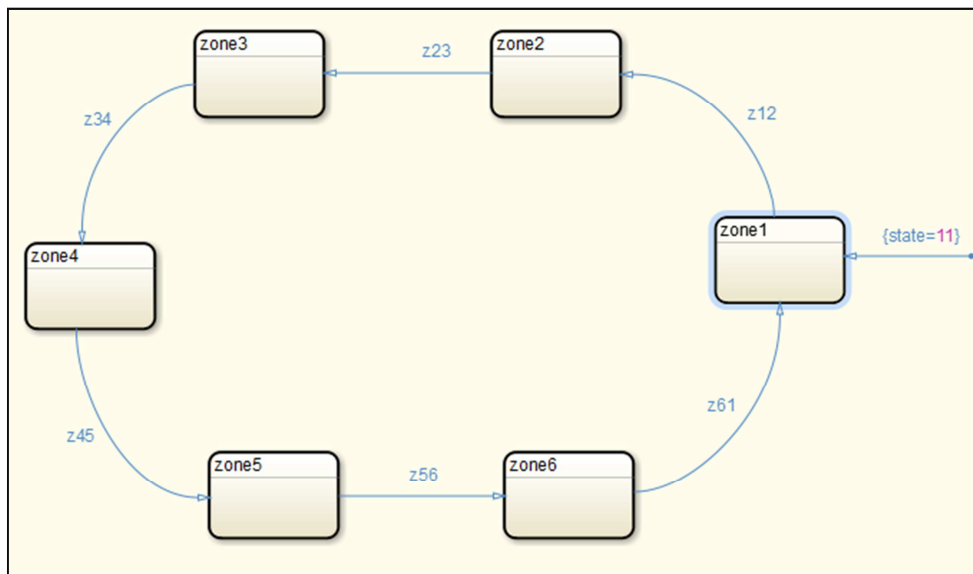
The controller receives at its inputs the uncontrollable events generated by the process and reacts to these events by

sending one of the controllable events on the entry of the interface A. The controller limits the evolution of the plant in

the intervals  $[\phi_{ref}^+, \phi_{ref}^-]$  for the stator flux and  $[\Gamma_{ref}^+, \Gamma_{ref}^-]$  for the electromagnetic torque.



(a)



(b)

Figure 8. a) Automaton modeling Controller b) Internal Architecture of controller.

6.1. Specification of Command

Initially, the flux and the torque are in state E11, the controller applies the command  $\vec{V}_{i+1}$  to increase the flux and the torque.

When the working point arrived in state E12, the controller applies the command  $\vec{V}_{i+2}$  to increase the torque and decrease the flux.

When the working point arrived in state E13, the controller applies the command  $\vec{V}_{i-1}$  to increase the flux and decrease the torque.

When the working point arrived in state E14, the controller applies the command  $\vec{V}_{i-2}$  to decrease the torque and the flux.

The evolution of the torque is limited in the interval  $[\Gamma_{ref}^+, \Gamma_{ref}^-]$  and the evolution of the flux is limited in the interval  $[\phi_{ref}^+, \phi_{ref}^-]$ .

The automata representing the controller and its internal architecture are given in figure 8, when the vector stator flux is in zone z1. In each state, a among the four vectors  $\vec{V}_{i+1}, \vec{V}_{i+2}, \vec{V}_{i-1}, \vec{V}_{i-2}$  is applied to maintain the evolution of

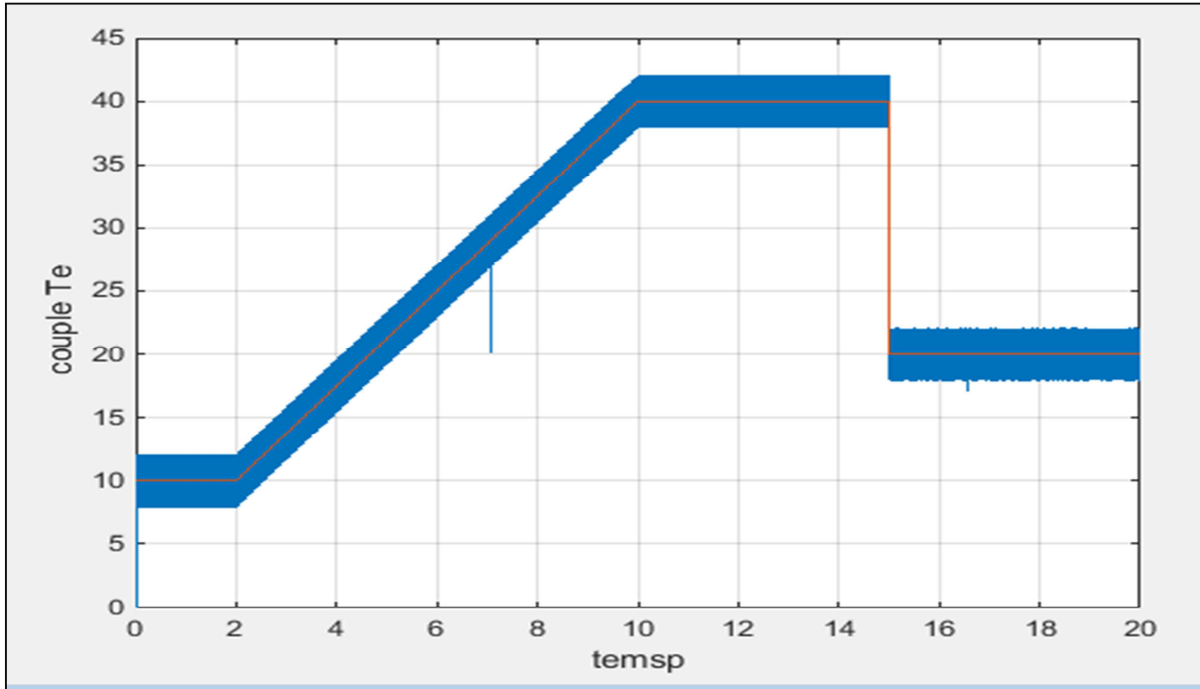
the flux and the torque to the inside of the fixed intervals according to the undulations tolerated.

environment Matlab/Simulink/stateflow (2014b). The ripples on the torque are fixed at 2Nm and 0.01wb for the stator flux.

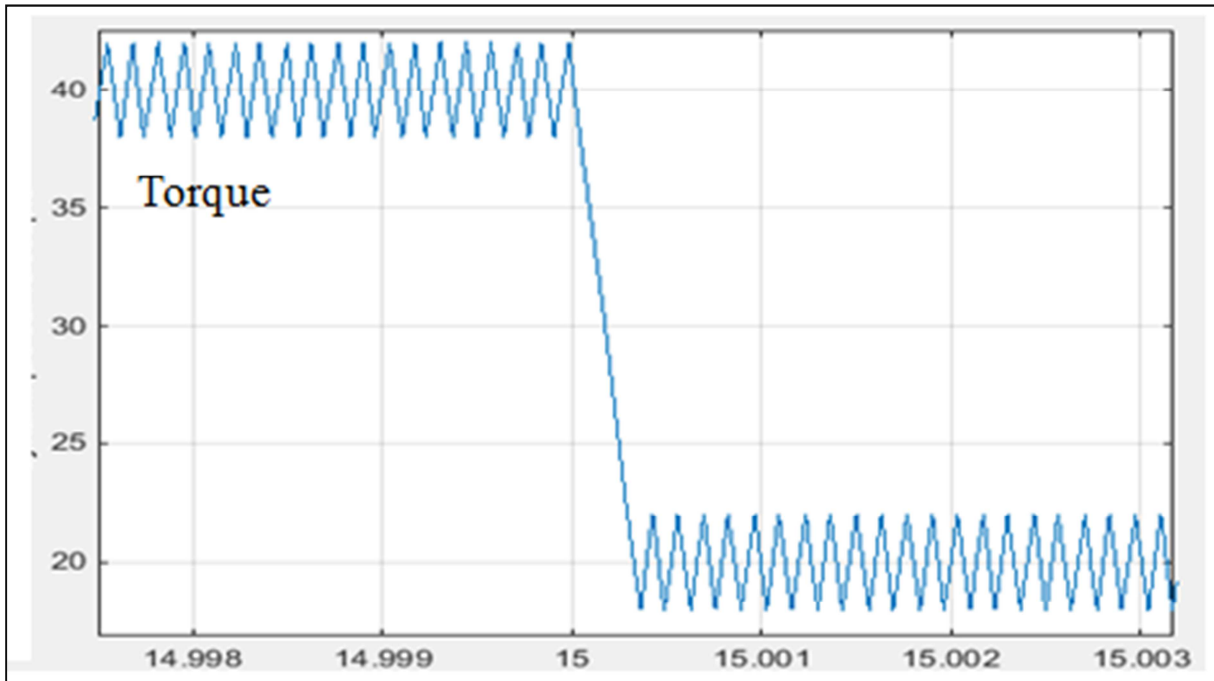
### 6.2. Simulation Results

The simulations are performed in the simulation

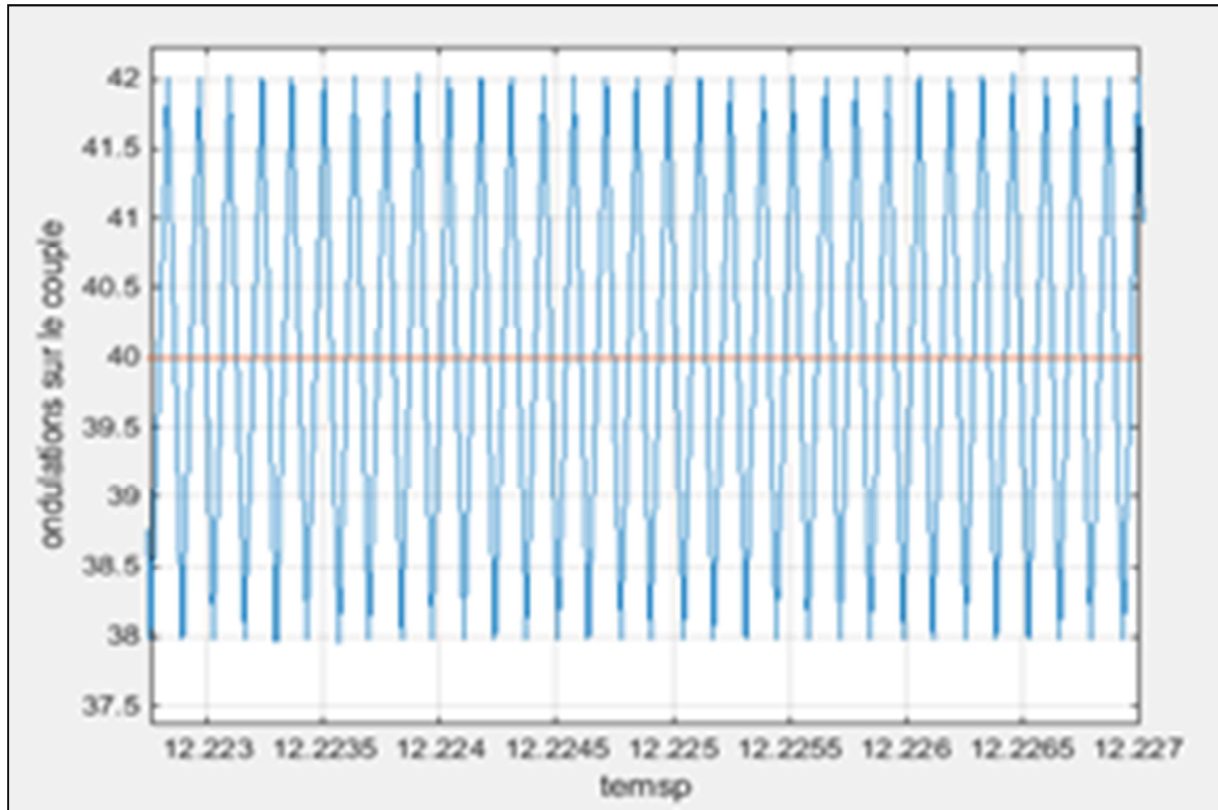
#### 6.2.1. Simulation of the Response of the Torque



(a)



(b)



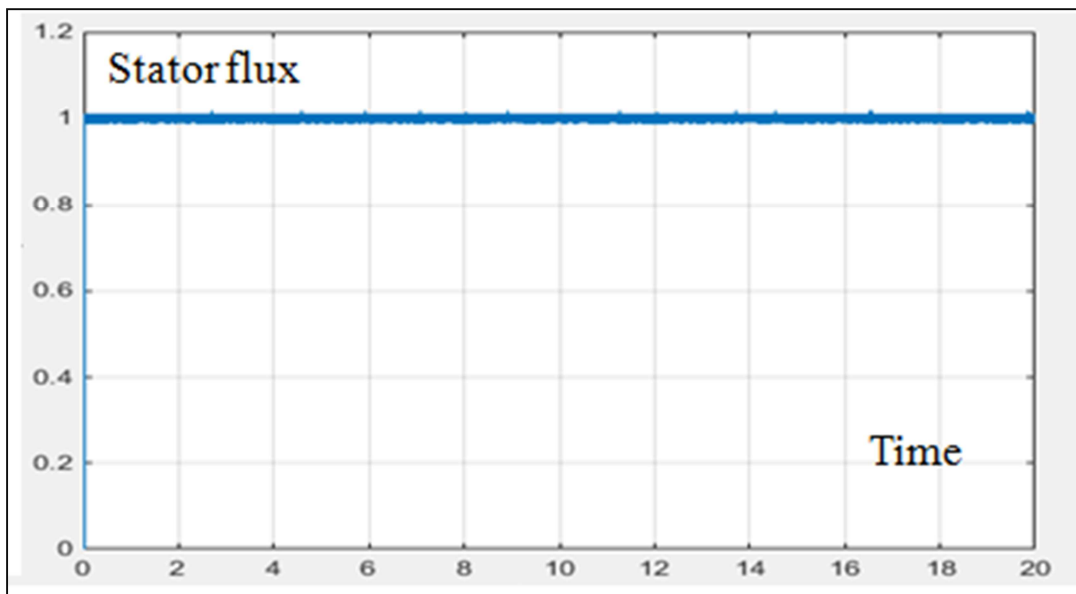
(c)

**Figure 9.** a) Simulation of the response of the torque b) The dynamic torque c) Ripples on the torque.

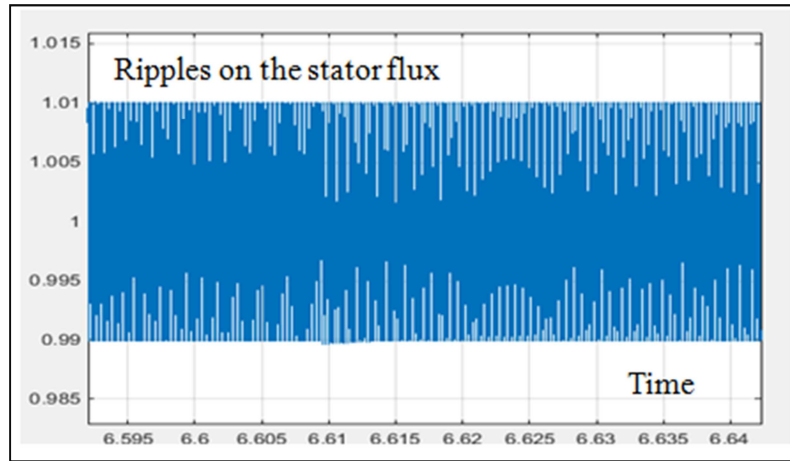
On figure 9(a), we observed the response of the torque which follows exactly the reference torque however the undulations on the torque are not reduced.

On figure 9 (b), the dynamics on the torque is represented for one level of 20Nm. We find exactly the results of the classical DTC.

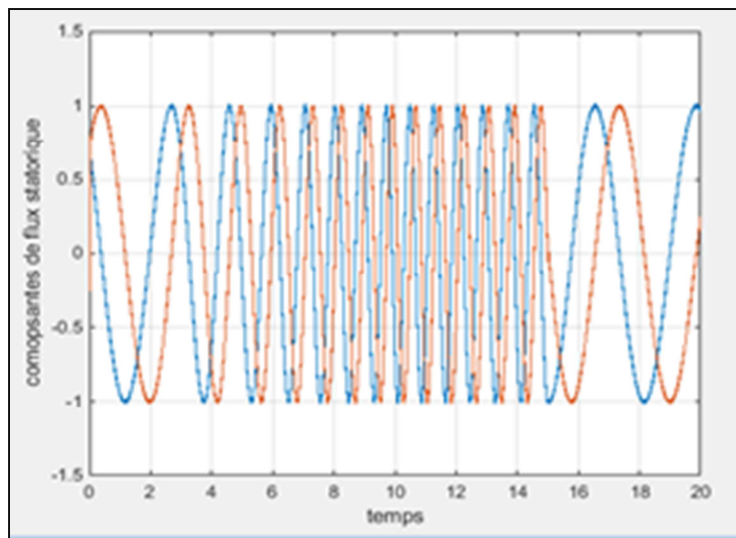
### 6.2.2. Simulation of the Response of the Flux



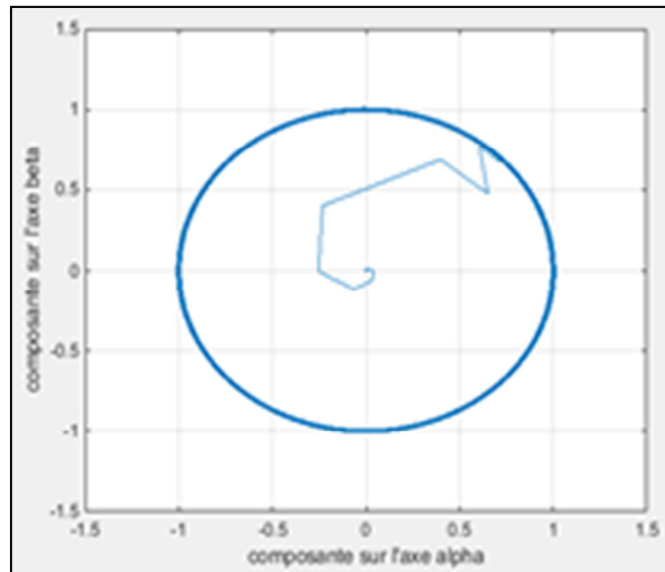
(a)



(b)



(c)



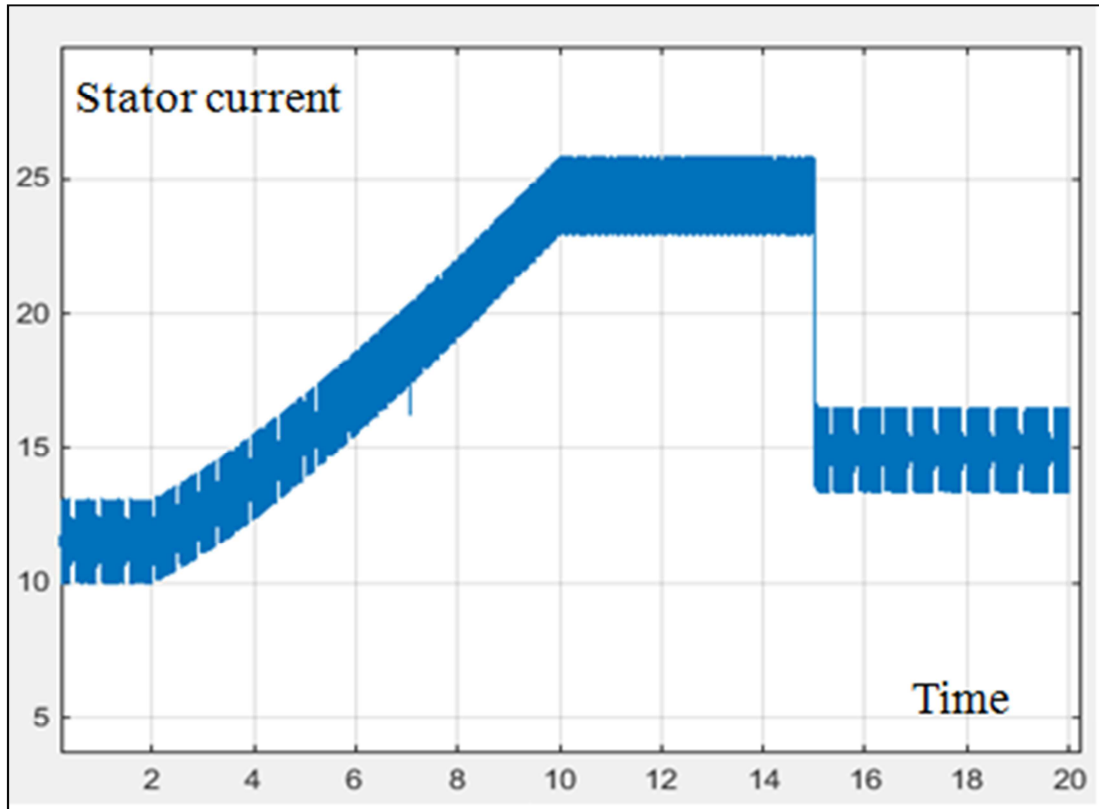
(d)

**Figure 10.** a) Response of the simulation of the stator flux b) Ripples on the flux c) Evolution of the flux components  $\phi_{s\alpha}$  and  $\phi_{s\beta}$  d) Evolution of the end of stator flux.

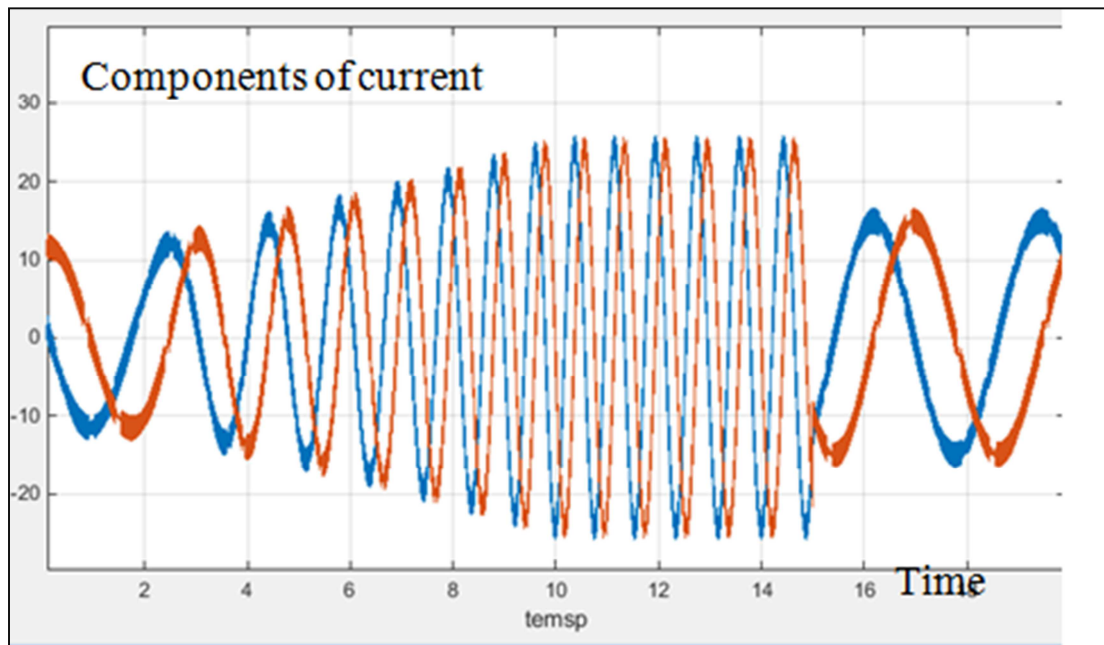
On figures 10 a, b, c, d, it represents the evolutions of the components of the stator flux. We find exactly the results of the classical command DTC.

The amplitude of flux remains constant, the end of the vector flux remains in a circular ring. The components  $\phi_{s\alpha}$  and  $\phi_{s\beta}$  are sinusoidally with a slight variation of frequency as a function of the amplitude of the reference torque. The ripples on the flux correspond to the variations tolerated on this grandeur.

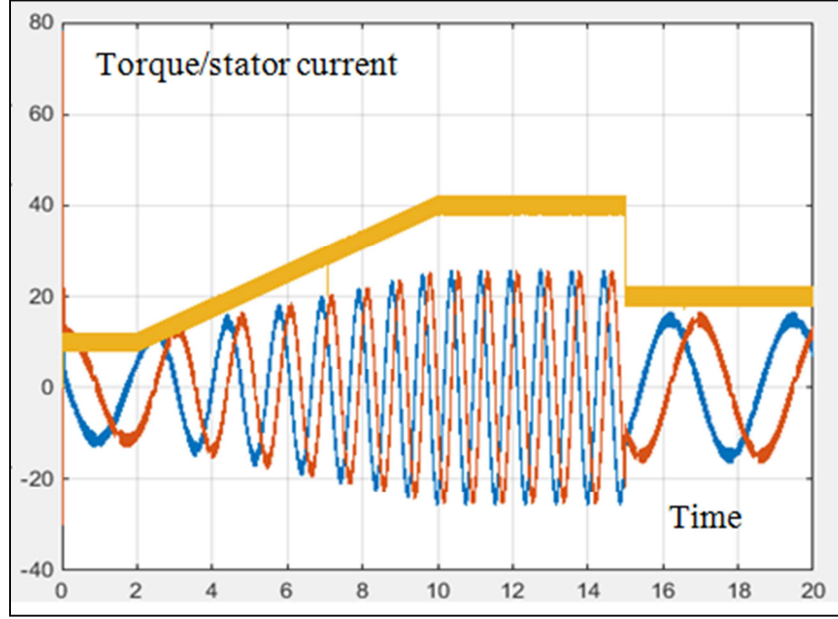
### 6.2.3. Simulation of the Response of the Courant



(a)



(b)



(c)

**Figure 11.** a) Simulation of the response of the stator current; b) Simulation of the response of the components of the current; c) Components of stator current as a function of the torque.

On figure 11, we can observe the response of the current which at the same form that the torque. The amplitudes of the components of the current follow the amplitude of the torque with a slight variation of the frequency.

## 7. Synthesis of a Controller with Reduction of Ripples on the Torque

### 7.1. Specification of Command

Our specification S requires to drive the DES {Inv-IM, A, G}, modeled by the 673-state automaton P of Section 5-2, into the set of regions  $\{R_{u,v}; u, v = 2, 3\}$  and to force it to remain into this set. S will thus consist of the following three requirements:

- 1) P, which is initially in the region  $R_{1,1}$ , must enter the set of regions  $\{R_{u,v}; u, v = 2, 3\}$ , i. e., the set of states  $\{(u; v); i)_k; u, v = 2, 3\}$ . Or equivalently: the plant must leave the set of regions  $\{R_{u,v}; (u=1) \vee (v=1)\}$ , i. e., the set of states  $\{(u; v); i)_k; (u=1) \vee (v=1)\}$ . This requirement is guaranteed by the following one: the event Null must never occur. Indeed, Null can occur only from a region in  $\{R_{u,v}; (u=1) \vee (v=1)\}$ , and can be avoided uniquely by driving IM to leave the set of regions  $\{R_{u,v}; (u=1) \vee (v=1)\}$ . In fact, the event Null has been introduced as a mean to express this first requirement.
- 2) After the plant enters a region  $R_{2,v}$  or  $R_{3,v}$ , then it never goes to a region  $R_{1,v}$  or  $R_{4,v}$ . Or equivalently: the events  $\phi_2^1$  and  $\phi_3^4$  must never occur.
- 3) After the plant enters a region  $R_{u,2}$  or  $R_{u,3}$ , then it never goes to a region  $R_{u,1}$  or  $R_{u,4}$ . Or equivalently: the events  $\Gamma_2^1$  and  $\Gamma_3^4$  must never occur.

To recapitulate, S simply forbids the following five (uncontrollable and unforcible) events Null,  $\phi_2^1$ ,  $\phi_3^4$ ,  $\Gamma_2^1$ ,  $\Gamma_3^4$ . S can be expressed as a single-state automaton with self loops of all the events of the alphabet  $\Sigma$  except the above five events. If we apply a synchronized product of P and S, we have the specification S' obtained from P by "cutting" the above five events.

### 7.2. Supervisor Synthesis

The inputs of the supervisor synthesis are:

- Automaton P modeling the plant (Sect. 5-2).
- Automaton S modeling the specification (Sect. 7-1).
- Controllability and forcibility of each event.

We have applied the synthesis procedure of the software tool TTCT [15]. With TTCT, forcible events can be forced to occur before an event tick that models the passing of one time unit. To be able to use TTCT, we have adapted P and S by preceding every unforcible event by the event tick. This adaptation is consistent with Hypothesis 5.1. The solution synthesized provides several possible scenarios of control. Here is the simplest one:

- Initially, we are in the initial state  $\langle 1; 1; 1 \rangle_0$ , that is: the flux and the torque are in Region  $R_{1,1}$ , the flux vector is in zone  $z_1$ , and the null control vector  $\vec{v}_0$  is applied.
- When a state  $\langle u; v; i \rangle_k$  such that  $u < 3$  and  $v < 3$  is reached and  $k \neq i+1$ , then Sup generates the event  $\vec{v}_{i+1}$ . Intuitively, when  $\phi_s < \phi_{wp}$  and  $\Gamma < \Gamma_{wp}$ , the control vector  $\vec{v}_{i+1}$  is applied to increase  $\phi_s$  and  $\Gamma$ . Note that this case applies to the initial state.
- When a state  $\langle 3; v; i \rangle_k$  such that  $v < 3$  is reached and  $k \neq i+2$ , then Sup generates the event  $\vec{v}_{i+2}$ . Intuitively,

when  $\varphi_s > \varphi_{wp}$  and  $\Gamma < \Gamma_{wp}$ , the control vector  $\vec{V}_{i+2}$  is applied to decrease  $\varphi_s$  and increase  $\Gamma$ .

- When a state  $\langle u; 3; i \rangle_k$  such that  $u < 3$  is reached and  $k \neq i-1$ , then Sup generates the event  $\vec{V}_{i-1}$ . Intuitively, When  $\varphi_s < \varphi_{wp}$  and  $\Gamma > \Gamma_{wp}$ , the control vector  $\vec{V}_{i-1}$  is applied to increase  $\varphi_s$  and decrease  $\Gamma$ .
- When a state  $\langle 3; 3; i \rangle_k$  is reached and  $k \neq i-2$ , then Sup generates the event  $\vec{V}_{i-2}$ . Intuitively, when  $\varphi_s > \varphi_{wp}$  and  $\Gamma > \Gamma_{wp}$ , the control vector  $\vec{V}_{i-2}$  is applied to decrease  $\varphi_s$  and  $\Gamma$ .

Note that Sup never generates an event  $\vec{V}_k$  that leads to a nondeterministic state  $\langle u; v; i \rangle_k$ , i. e., such that  $k = i$  or  $k = i+3$ . Nevertheless, a nondeterministic state can be reached by an event  $z_{i-1}^i$  or  $z_{i+1}^i$ . When such a situation occurs, Sup has not a real control on  $\Gamma$ , because it is not known whether  $\Gamma$  increases or decreases. Sup will quit such a nondeterministic

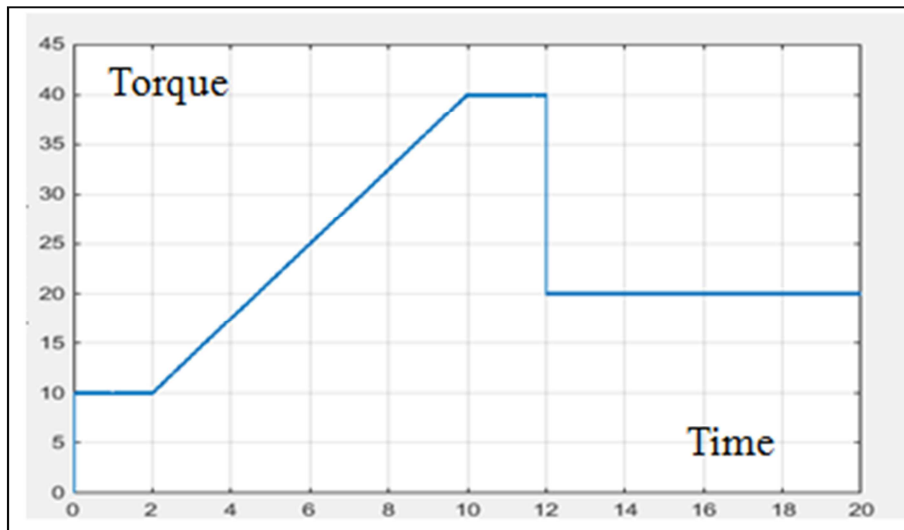
situation by generating one of the four control vectors  $\vec{V}_{i-2}$ ,  $\vec{V}_{i-1}$ ,  $\vec{V}_{i+1}$ ,  $\vec{V}_{i+2}$ , depending on whether each of  $\varphi_s$  and  $\Gamma$  must be increased or decreased.

### 7.3. Simulation Results

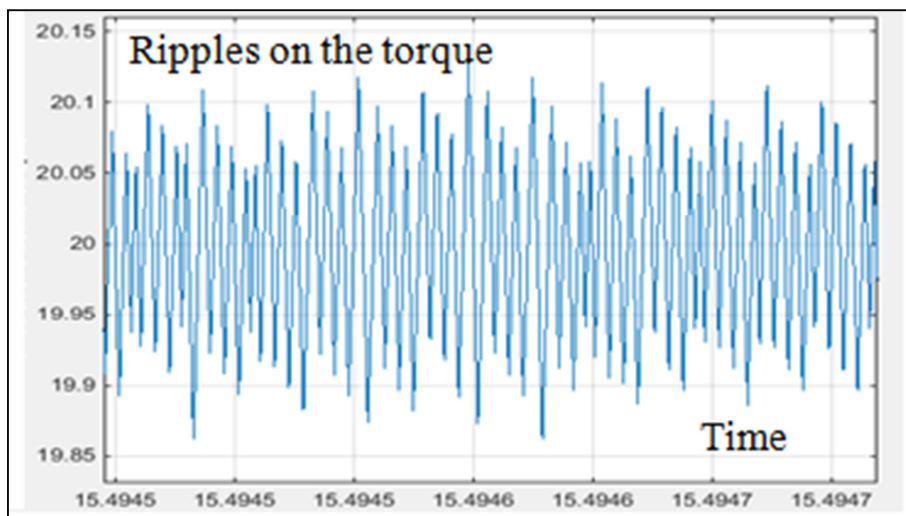
We present in this part the numerical simulation results, illustrating the behavior of the structure of direct torque control applied to an induction motor. The simulations are performed for a sampling period  $T_e$  equal to  $1\mu s$ .

Figures 12, 13 shows the responses of the electromagnetic torque and the stator currents  $i_{s\alpha}$  and  $i_{s\beta}$  for reference torque which varies according to figure 11, we can note the very good performance of the torque which precisely follows its reference.

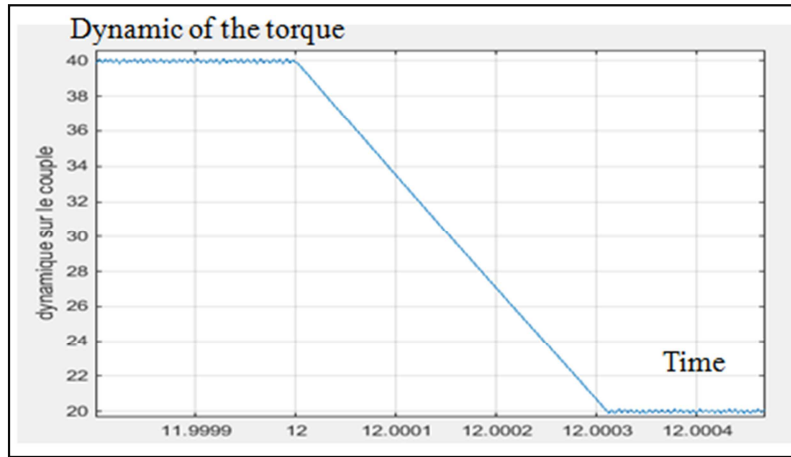
#### 7.3.1. Simulation of the Response of the Courant



(a)



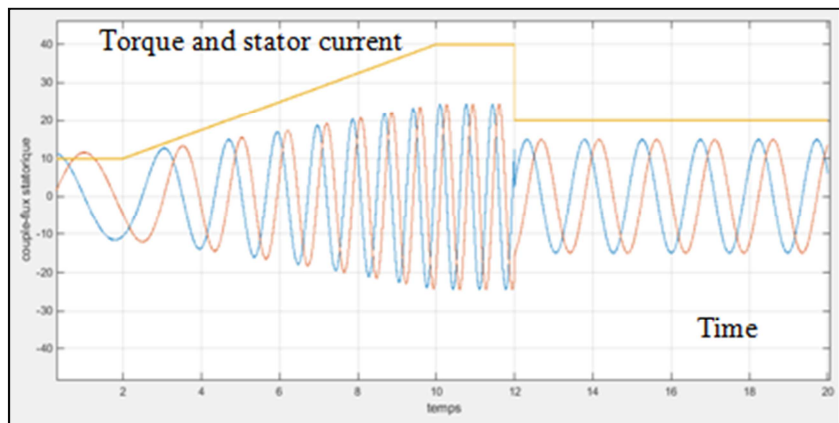
(b)



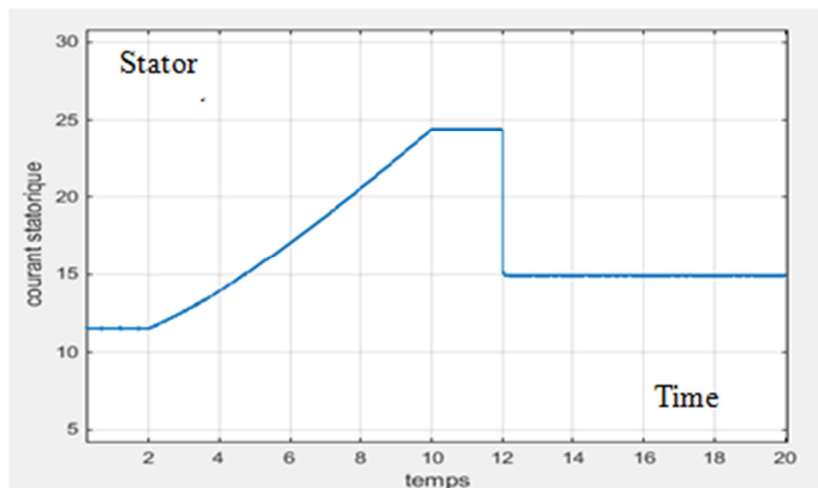
(c)

Figure 12. a) Simulation of the response of the torque b) Ripples on the torque c) dynamique of torque.

7.3.2. Simulation of the Response of the Stator Current



(a)

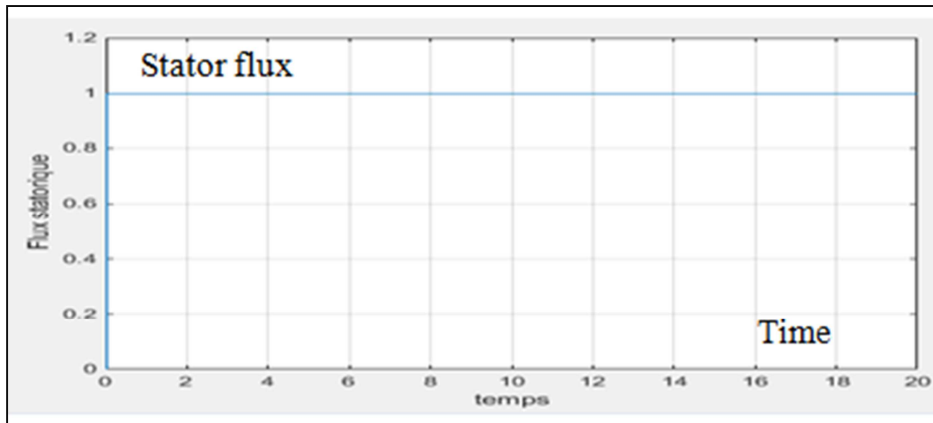


(b)

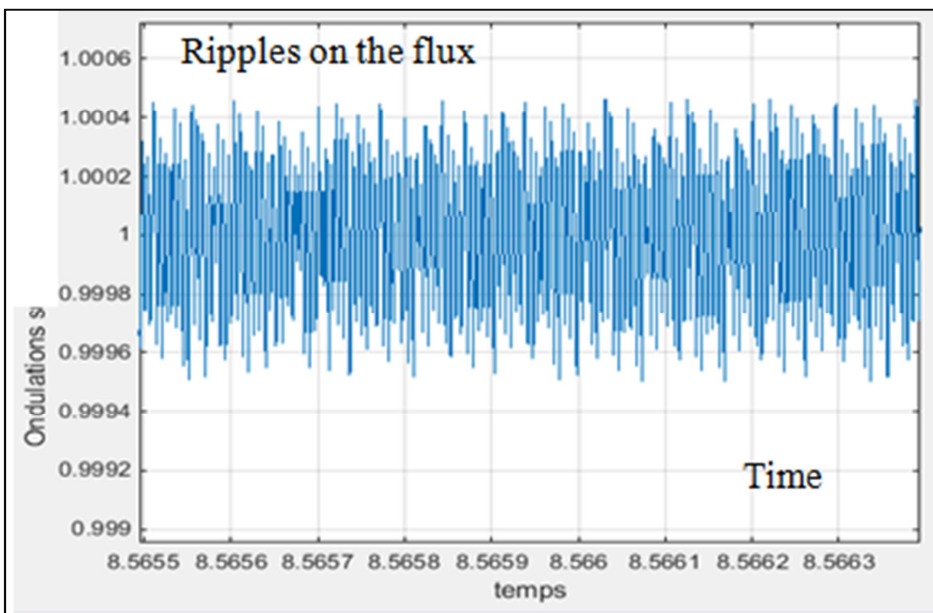
Figure 13. a) Simulation of the response of the current as a function of the reference torque b) Amplitude of the stator current.

The stator currents  $i_{sa}$  and  $i_{sb}$  respond well to the changes imposed on the torque. It is observed that the stator current retains a very close form of sinusoid for all torque variations. We also notice that the stator current is rapidly established in the phase of transition without a great overcurrent.

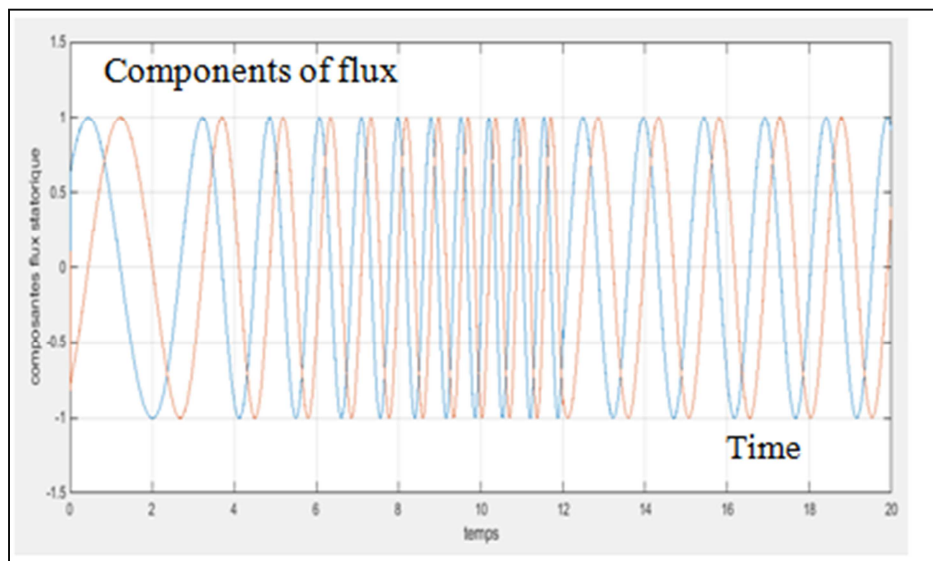
7.3.3. Simulation of the Response of the Flux



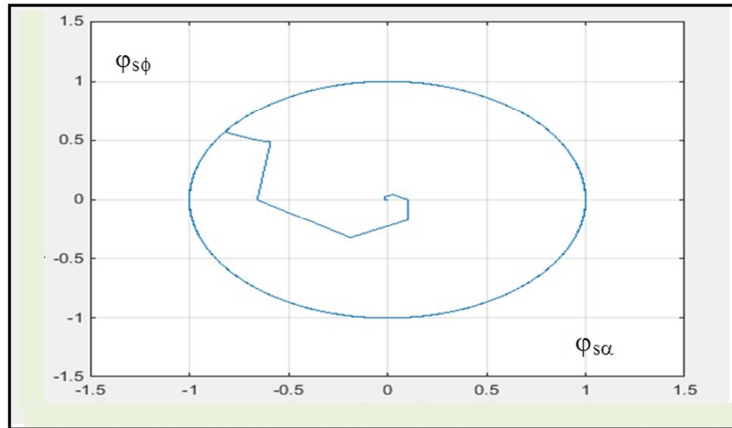
(a)



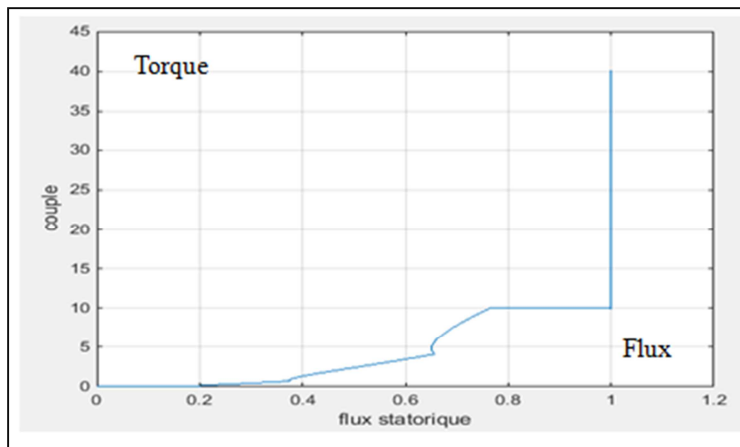
(b)



(c)



(d)



(e)

**Figure 14.** a) Evolution of amplitude of the stator flux b) Undulations on the stator flux c) Simulation of the response of the components of the stator flux d) The trajectory of the end of the vector stator flux e) Evolution of the working point.

On figure 14, we observed the response of stator flux for the reference of the given torque. The flux varies around the predefined value (1wb) with ripples very low. The end of the vector stator flux describes a circular path; it is maintained constant, which allows controlling the electromagnetic torque (decoupling flux-torque). We find exactly the results of the classical structure of the direct torque control with the

advantage that the ripples on the torque are much reduced.

We note a slight variation of frequency of the components of the stator flux (principle of the DTC control). We can also observe the dynamics on the torque; it is efficient compared to Classic commands.

**7.3.4. Simulation of the Response of the Zone**

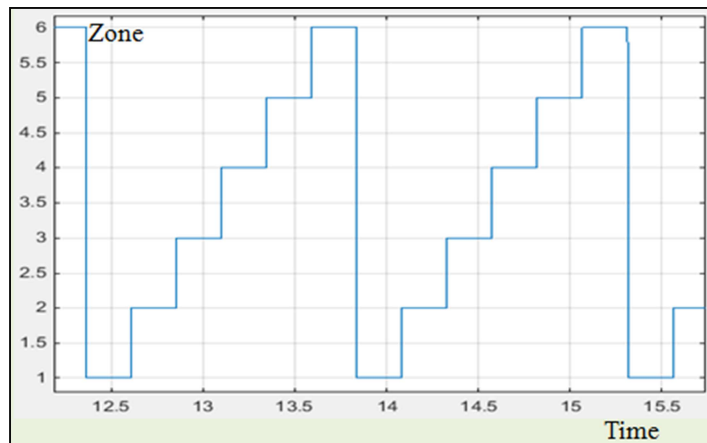


**Figure 15.** Evolution of the vector stator flux.

## 8. Conclusion

In this paper, we have studied the Direct Torque Control (DTC) of an Induction Motor coupled to an Inverter (Inv-IM). DTC permits to control directly the stator flux and the torque by selecting the appropriate inverter state. Our first contribution is the modeling of Inv-IM as a hybrid system (HS), where the inverter is modeled as a discrete event system (DES) and the induction motor is modeled as a continuous system. Our second contribution is the abstraction of the continuous dynamics of the induction motor as a DES. The HS is thus modeled as a DES. The advantage of this abstraction is that all the rigorous analysis and design methods for DES can be applied for studying DTC. Our third contribution is the use of Supervisory Control Theory (SCT) of DES to drive Inv-IM to a desired working point.

For the sake of clarity, we have based all our study on the fact that the targeted working point is an interval of stator flux and an interval of torque. But our study can be easily adapted for other working points, for example moving the head of the stator flux vector in a circular ring.

An interesting previous work has been done in [16], [17], but the specification was defined with an a priori knowledge of the solution and was not defined as the most permissive solution. Besides, no solution was proposed to the nondeterminism of the 6-zone division. In the present paper, these limitations are solved by taking more advantage of SCT.

As a future work, we intend to improve our control method by using a hierarchical control and a modular control, which are very suitable to take advantage of the fact that the event model of the plant has been constructed hierarchically and modularly. Indeed:

- The hierarchy is in two levels in the construction of the plant. In a first level, the inverter is modeled by a 7-state automaton  $A$ , whose states  $\{q_k: k=1\dots6\}$  corresponds to the application of the control vectors  $\vec{V}_k: k=1\dots6$ . In a second level, each state  $q_k$  is replaced by an automaton  $M_k$  modeling the behavior of the induction motor under the control of  $\vec{V}_k$ .
- The modularity is used when constructing each subautomaton  $M_k$  of the plant by combining a 16-state and 6-state automata.

## References

- [1] A. A. Pujol. Improvements in direct Control of Induction Motors. PhD thesis, Department of Electronical engineering, Polytechnical University of Catalunya, Terrassa, Spain, November 2000.
- [2] J. L. Romeral. Optimizaci' on de Modelos de Control Digital para Motores (AC). PhD thesis, Department of Electronical Engineering, Polytechnical University of Catalunya, Terrassa, Spain, June 1995.
- [3] D. Bedford. Control Vectorial Adaptativo de Motores As' incronos de Inducci' on. PhD thesis, Department of Electronical Engineering, Polytechnical University of Catalunya, Terrassa, Spain, October 1999.
- [4] S. Yamamura. AC Motors for high-performance applications. Analysis and Control. Marcel Dekka, Inc., 1986.
- [5] I. Takahashi and T. Noguchi. A new quick response and high efficiency control strategy of induction motors. IEEE Transactions on Industry Applications, 22(5): 820–827, Sept.-Oct. 1986.
- [6] I. Takahashi and S. Asakawa. Ultra-wide speed control of induction motor covered 10 a 6 range. IEEE Transactions on Industry Applications, 25: 227–232, 1987.
- [7] I. Takahashi and T. Kanmashi. Ultra-wide speed control with a quick torque response AC servo by DSP. In EPE, pages 572–577, Firenze, Italy, 1991.
- [8] T. G. Habetler and D. M. Divan. Control strategies for direct torque control using discrete pulse modulation. IEEE Transactions on Industry Applications, 7(5): 893–901, 1991.
- [9] P. J. Ramadge and W. M. Wonham. The control of discrete event systems. Proc. IEEE, 77: 81–98, January 1989.
- [10] I. Boldea and S. A. Nasar. Vector Control of AC Drives. CRC Press Inc., 1992.
- [11] P. Vas. Sensorless Vector and Direct Torque Control of AC Machine. Oxford Univ. Press, London, U. K., 1998.
- [12] I. Takahashi and S. Ohimori. High performance direct torque control of an induction motor. IEEE Transactions on Industry Applications, 25 (2): 257–264, 1989.
- [13] I. Ludtke. The Direct Control of Induction Motors. PhD thesis, Department of Electronics and Infomation Technology, Polytechnical University of Glamorgan, Wales, U. K., May 1998.
- [14] C. H. Golaszewski and P. J. Ramadge. Control of discrete event processes with forced events. In 26th CDC, pages 247–251, Los Angeles, CA, USA, 1987.
- [15] TTCT. Developed by the Systems Control Group of the University of Toronto. Downloadable from: <http://www.control.toronto.edu/people/profs/wonham/wonham.html>.
- [16] H. Yantour, J. Saadi, and A. Khoumsi. Modélisation et simulation d'une commande directe du couple appliquée à la machine asynchrone (DTC). In 6<sup>me</sup> conf. francophone de MOdélisation et Simulation (MOSIM), Rabat, Morocco, April 2006.
- [17] H. Yantour, J. Saadi, H. Medromi, and A. Khoumsi. An Event Approach to Model Direct Torque Control (DTC). In 2nd Int. Symposium on Communications, Control and Signal Processing (ISCCSP), Marrakesh, Morocco, March 2006.
- [18] L. Ghomri. Synthèse de contrôleur de systèmes hybrides à flux continu par réseaux de Petri hybrides, universite abou-bekr belkaïd – tlemcen faculte de genie électrique et électronique, 2012.
- [19] Mathilde Machin, J. Guiochet, David Powell, Helene Waeselynck, Introduction à la synthèse de superviseur, <https://hal.archives-ouvertes.fr/hal-00804879>, Submitted on 26 Mar 2013.

- [20] Andra Ioana Vasiliu, Synthèse de contrôleurs des systèmes à événements discrets basée sur les réseaux de Petri, <https://tel.archives-ouvertes.fr/tel-00767421>, Submitted on 19 Dec 2012